

Supplementary information

**Protein engineering of multi-enzyme virus-like particle
nanoreactors for enhanced chiral alcohol synthesis**

Taotao Feng,^{1,‡} Jiaxu Liu,^{1,‡} Xiaoyan Zhang,^{1,‡} Daidi Fan², and Yunpeng Bai^{1,*}

¹State Key Laboratory of Bioreactor Engineering, Shanghai Collaborative Innovation
Center for Biomanufacturing, East China University of Science and Technology,
Shanghai 200237, China

²Shaanxi R&D Centre of Biomaterials and Fermentation Engineering, School of
Chemical Engineering, Northwest University, Xi'an, Shaanxi 710069, China

*Corresponding author: Yunpeng Bai, ybai@ecust.edu.cn

‡These authors contributed equally.

Contents

1. Figures and tables

Figure S1. Michaelis-Menten kinetic assessments of SsCR and BmGDH encapsulated in the wild-type P22-SP-BmGDH-SsCR nanoreactors.

Figure S2. Expression and characterization of SP-*BmGDH-SsCR*.

Figure S3. SDS-PAGE of pure SsCR by nickel ion affinity chromatography.

Figure S4. SDS-PAGE of pure *BmGDH* by nickel ion affinity chromatography.

Figure S5. Schematic diagram of protein engineering of P22-SP-*BmGDH-SsCR*.

Figure S6. Rescreening the activity of SsCR and *BmGDH* in 24 variants of the nanoreactor P22-SP-*BmGDH-SsCR* M0.

Figure S7. Michaelis-Menten kinetic assessments of SsCR and *BmGDH* encapsulated in M0-M5.

Figure S8. Michaelis-Menten kinetic assessments of SsCR and *BmGDH* in V0-V5.

Figure S9. Conversion of **1a** by the nanoreactors P22-SP-*BmGDH-SsCR* (M0 and M5) and the fusion proteins SP-*BmGDH-SsCR* (V0 and V5).

Figure S10. Characterization of P22-SP-*BmGDH-SsCR* M0.

Table S1. Catalytic efficiency of M0 variants toward **1a** and glucose.

Table S2. Turnover frequency of SP-*BmGDH-SsCR* variants with **1a** and glucose.

Table S3. Michaelis-Menten kinetic analysis of SsCR and *BmGDH* in M0–M5.

Table S4. Michaelis-Menten kinetic analysis of SP-*BmGDH-SsCR* variants.

Table S5. Michaelis-Menten kinetics analysis of *BmGDH* variants.

Table S6. Michaelis-Menten kinetics analysis of SsCR variants.

Table S7. GC conditions used to determine the enantioselectivity of products.

2. GC spectra

1. Figures and tables

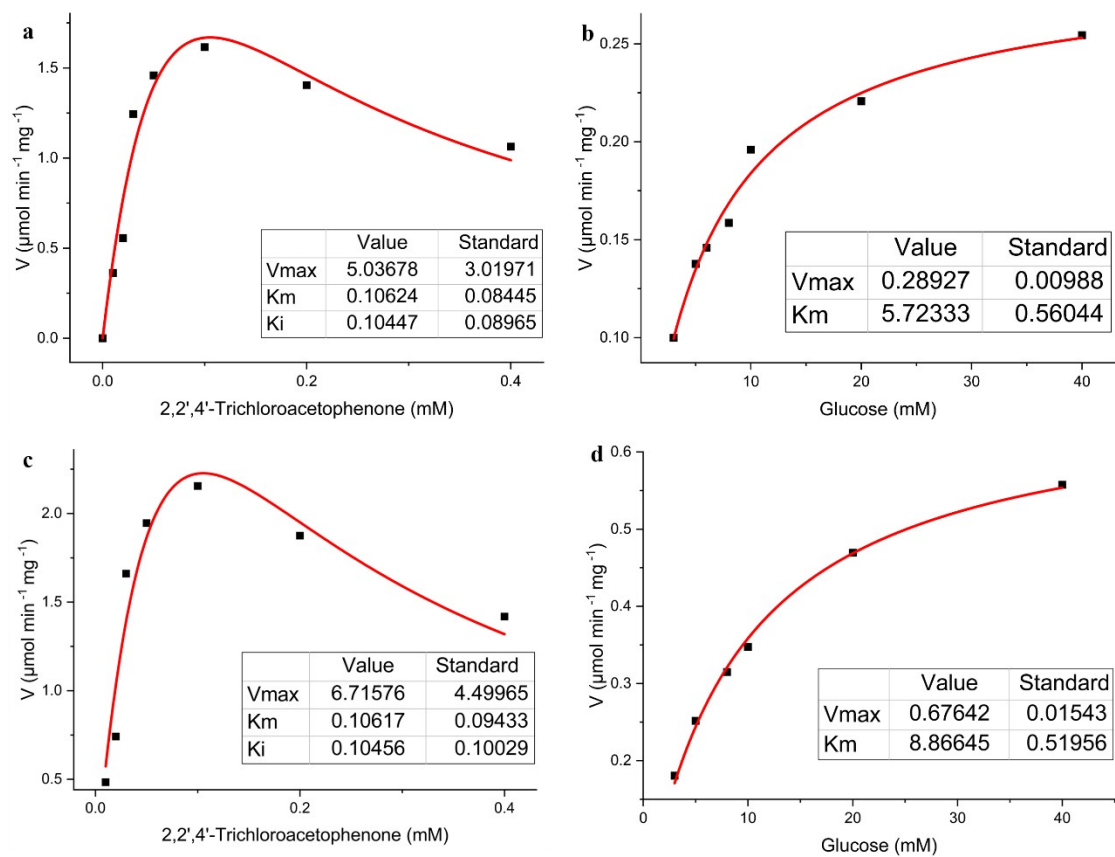


Figure S1. Michaelis-Menten kinetic assessments of *SsCR* and *BmGDH* encapsulated in the wild-type P22-SP-*BmGDH-SsCR* nanoreactors assembled from *E. coli* BL21 (DE3) bearing single plasmid (a) (b) and double plasmids (c) (d).

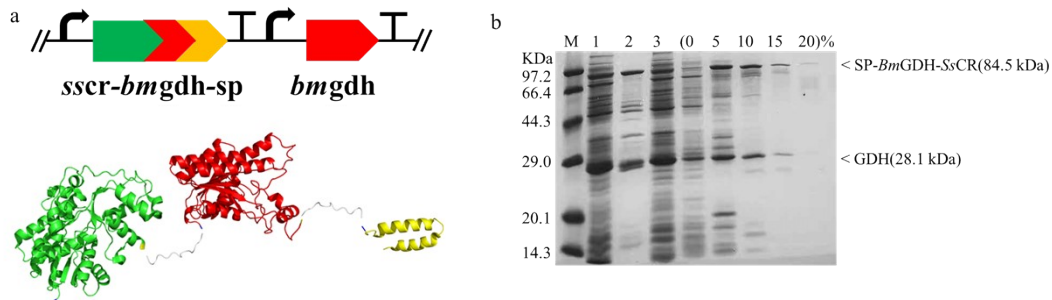


Figure S2. Expression and characterization of SP-*BmGDH-SsCR*. (a) Schematic of plasmids for the expression of SP-*BmGDH-SsCR*. (b) SDS-PAGE analysis of SP-*BmGDH-SsCR*. Lanes: M, protein marker; 1 and 2, the supernatant and precipitate obtained from cell lysis; 3, flow-through of protein; 0-20%: elution conditions with different volume ratios of buffer B in the mixed solution of buffer B and buffer A. Buffer A: 20 mM imidazole, 0.5 M NaCl and 20 mM Tris-HCl buffer, pH 7.4; Buffer B: 500 mM imidazole, 0.5 M NaCl and 20 mM Tris-HCl buffer.

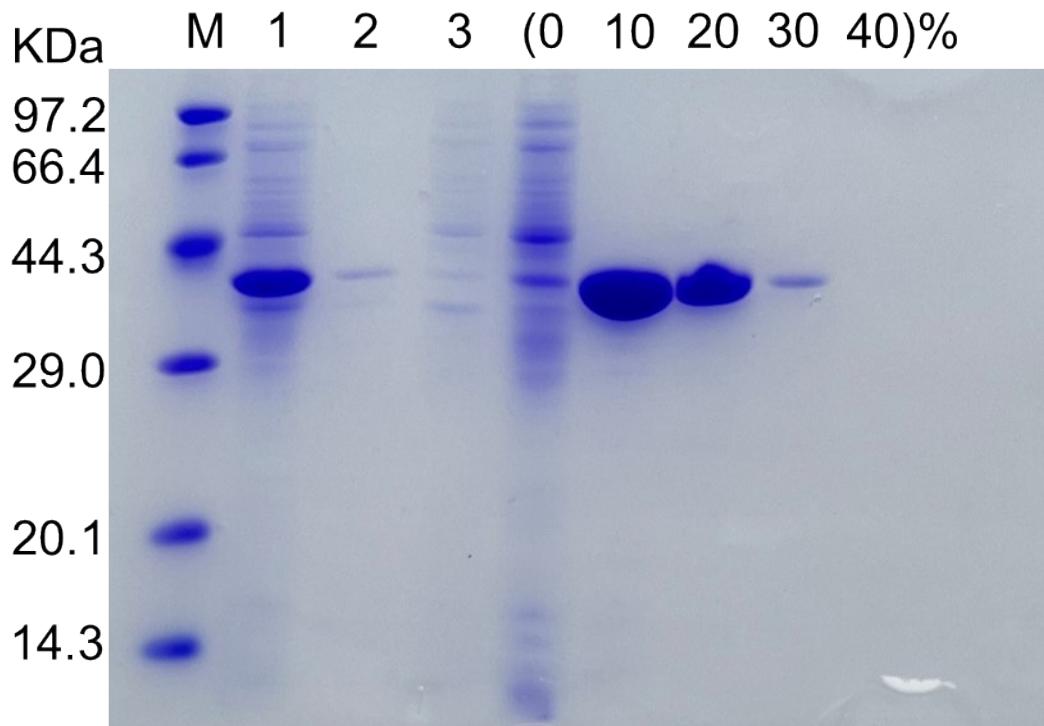


Figure S3. SDS-PAGE of pure *SsCR* by nickel ion affinity chromatography. M, Protein standard marker; 1, supernatant of cell lysate; 2, precipitant of cell lysate; 3, flow-through of protein; 0-40%: elution conditions with different volume ratios of buffer B in the mixed solution of buffer B and buffer A. Buffer A: 20 mM imidazole, 0.5 M NaCl and 20 mM Tris-HCl buffer, pH 7.4; Buffer B: 500 mM imidazole, 0.5 M NaCl and 20 mM Tris-HCl buffer.

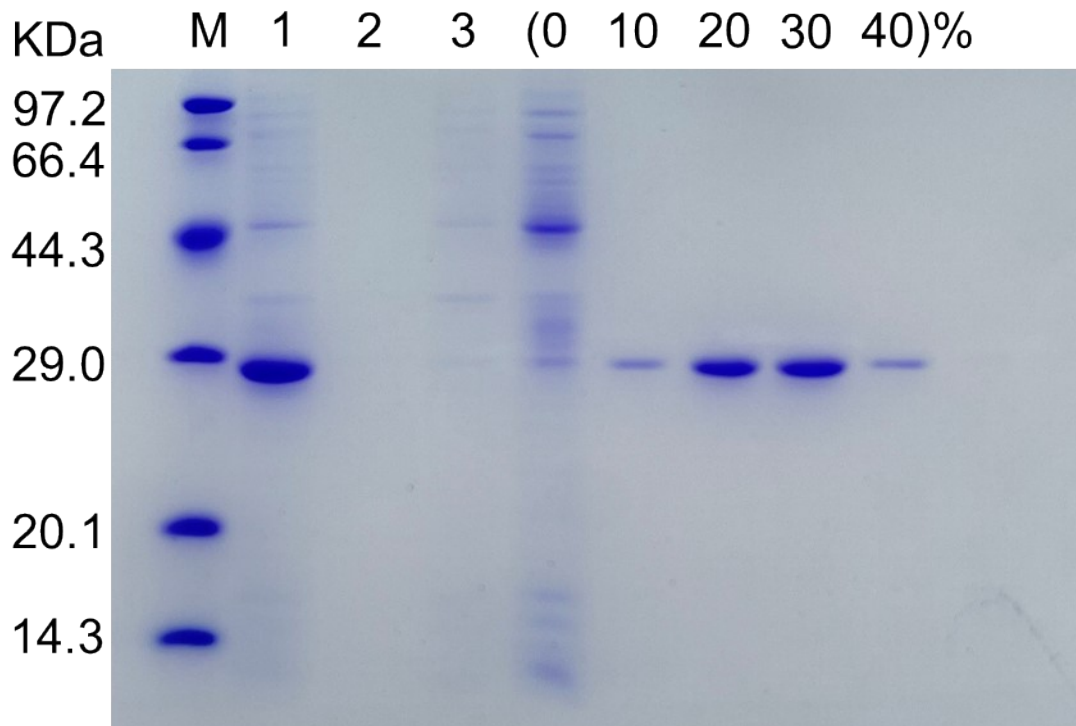


Figure S4. SDS-PAGE of pure *BmGDH* by nickel ion affinity chromatography. M, Protein standard marker; 1, supernatant of cell lysate; 2, precipitant of cell lysate; 3, flow-through of protein; 0-40%: elution conditions with different volume ratios of buffer B in the mixed solution of buffer B and buffer A. Buffer A: 20 mM imidazole, 0.5 M NaCl and 20 mM Tris-HCl buffer, pH 7.4; Buffer B: 500 mM imidazole, 0.5 M NaCl and 20 mM Tris-HCl buffer.

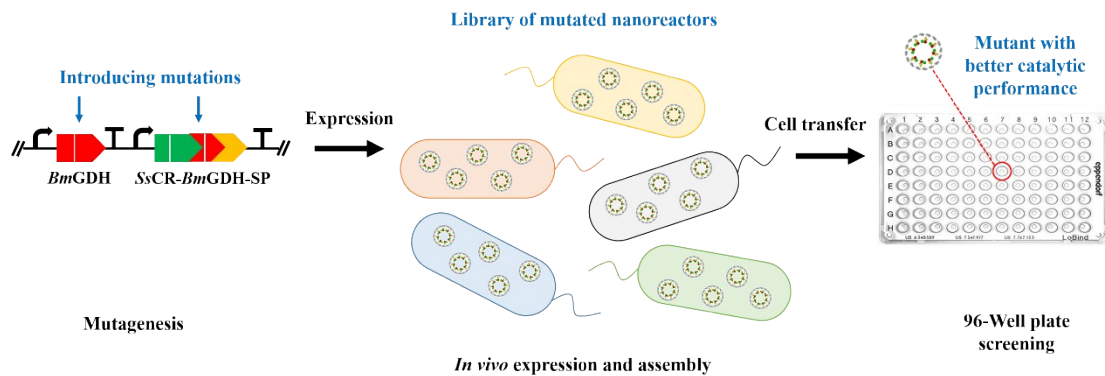


Figure S5. Schematic diagram of protein engineering of P22-SP-*BmGDH-SsCR*. Error-prone PCR was applied to both *BmGDH* and *SsCR-BmGDH-SP* to introduce mutations (white lines) in the plasmid. The mutated genes were transferred into *E. coli* BL21 (DE3) for the expression and self-assembly of P22-SP-*BmGDH-SsCR* nanoreactors. The single cell colonies of *E. coli* were cultured in agar plate and then transferred into 96-plate well. Cells were lysed and substrate was added for the screening of catalytic activity.

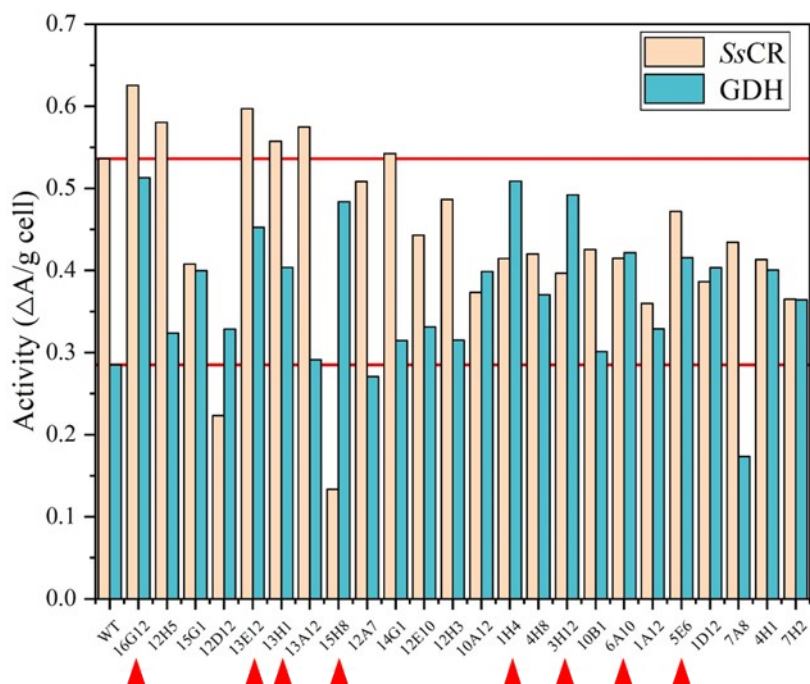
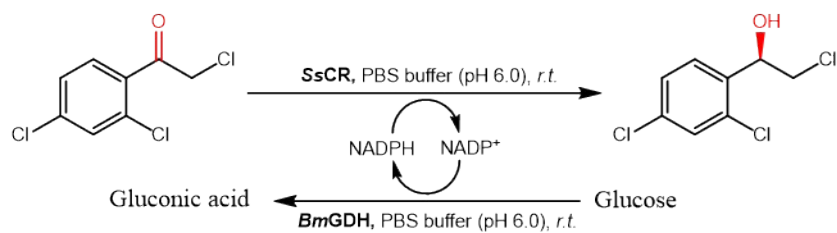
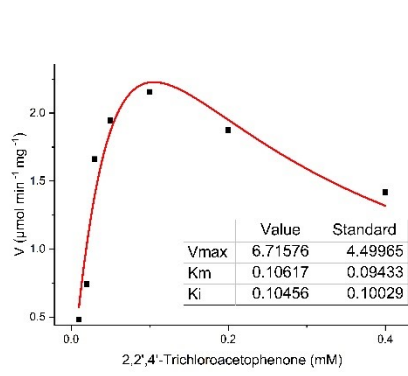
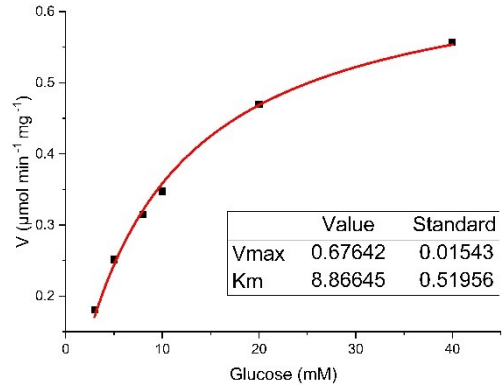


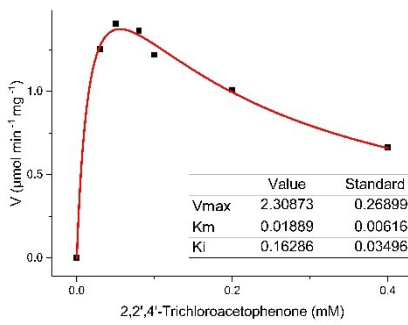
Figure S6. Rescreening the activity of *SsCR* and *BmGDH* in 24 variants of the nanoreactor P22-SP-*BmGDH*-*SsCR* M0. The arrows indicate the better variants which were subsequently used for sequencing.



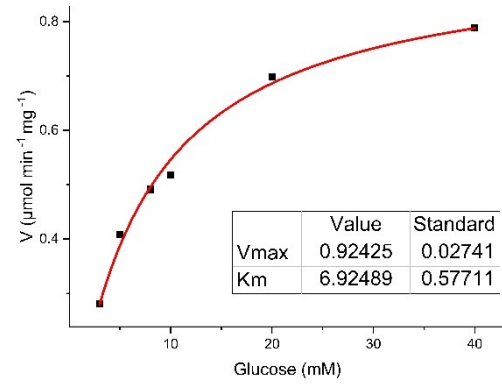
M0-SsCR



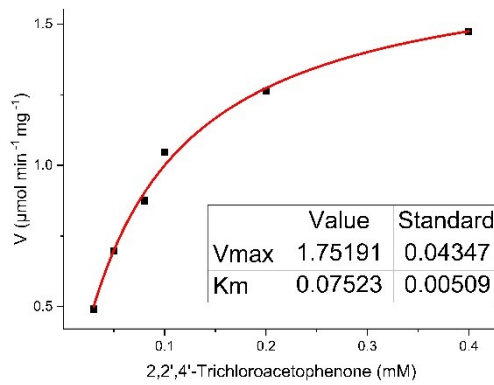
M0-BmGDH



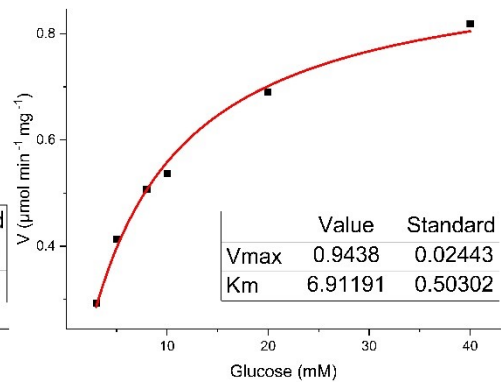
M1-SsCR



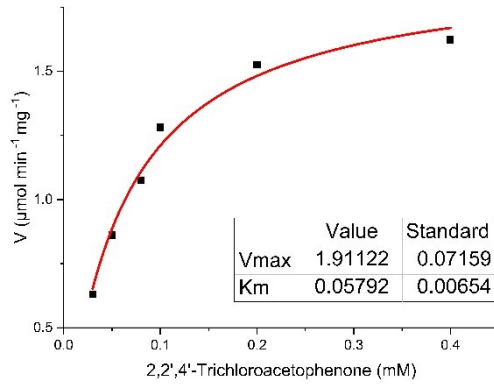
M1-BmGDH



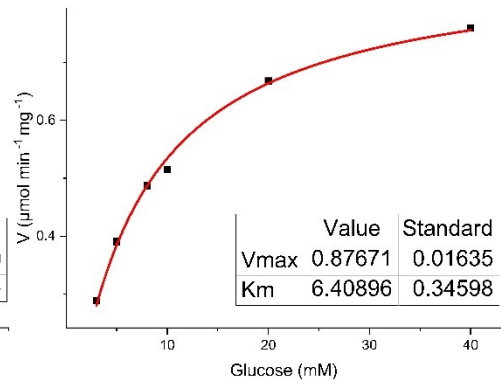
M2-SsCR



M2-BmGDH



M3-SsCR



M3-BmGDH

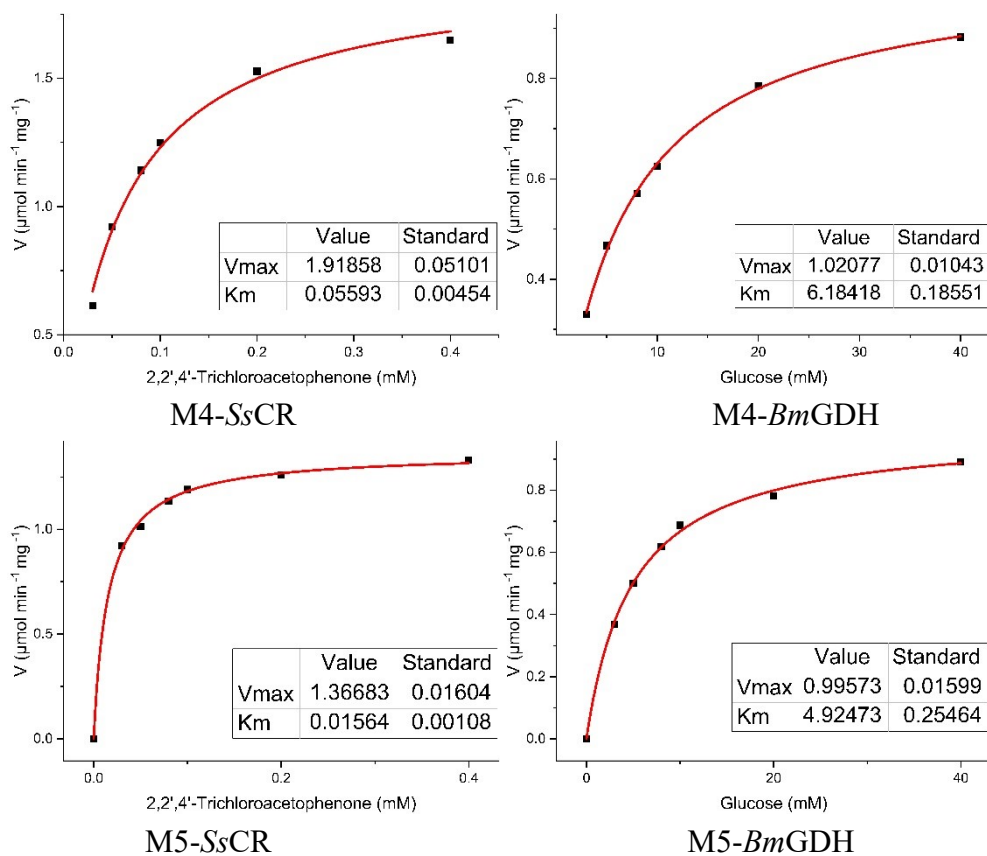
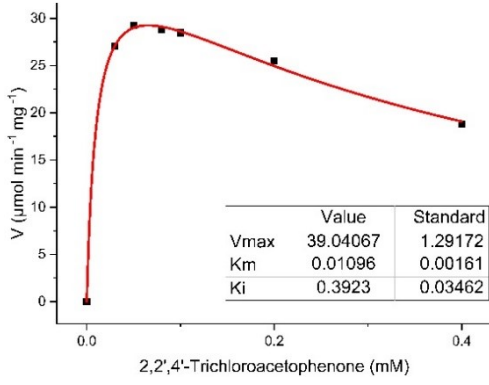
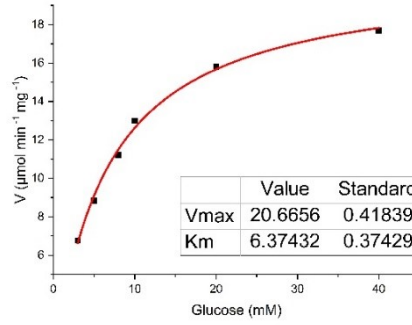


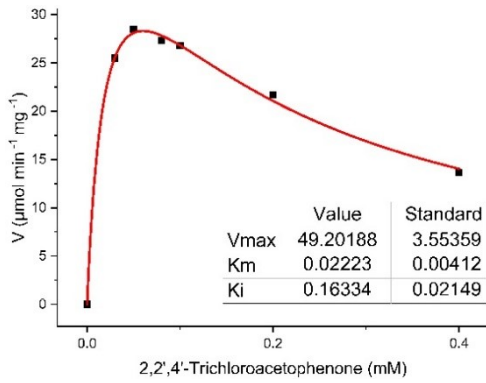
Figure S7. Michaelis-Menten kinetic assessments of *SsCR* and *BmGDH* encapsulated in M0-M5.



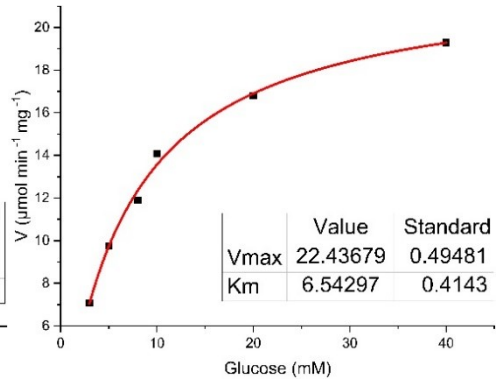
V0-SsCR



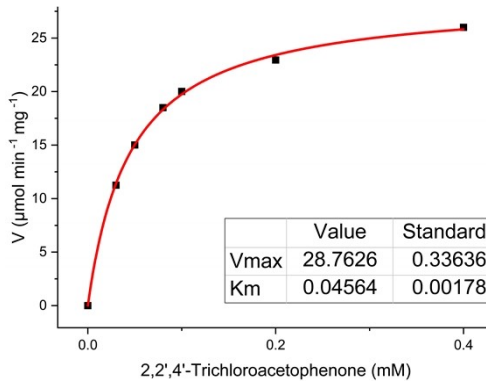
V0-BmGDH



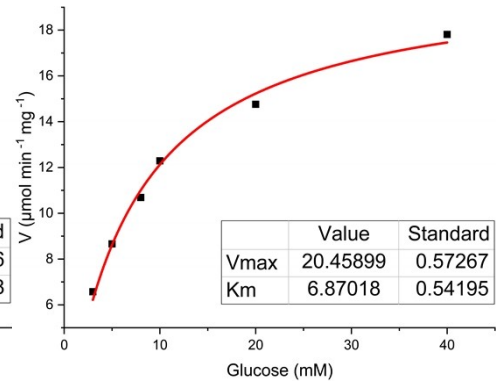
V1-SsCR



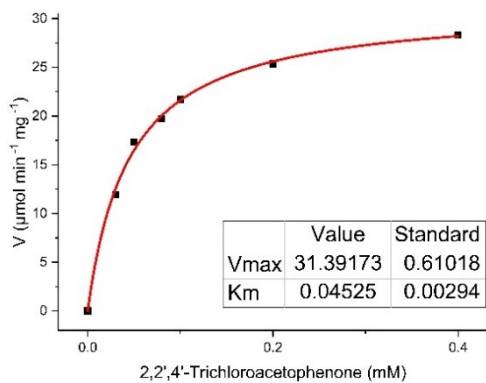
V1-BmGDH



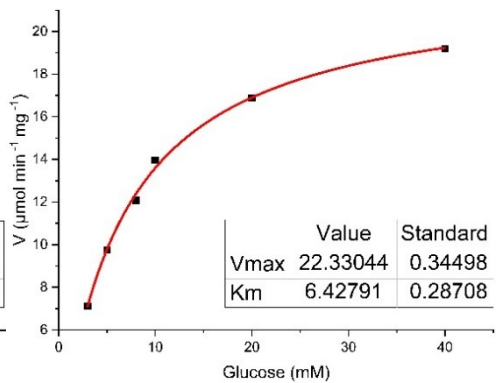
V2-SsCR



V2-BmGDH



V3-SsCR



V3-BmGDH

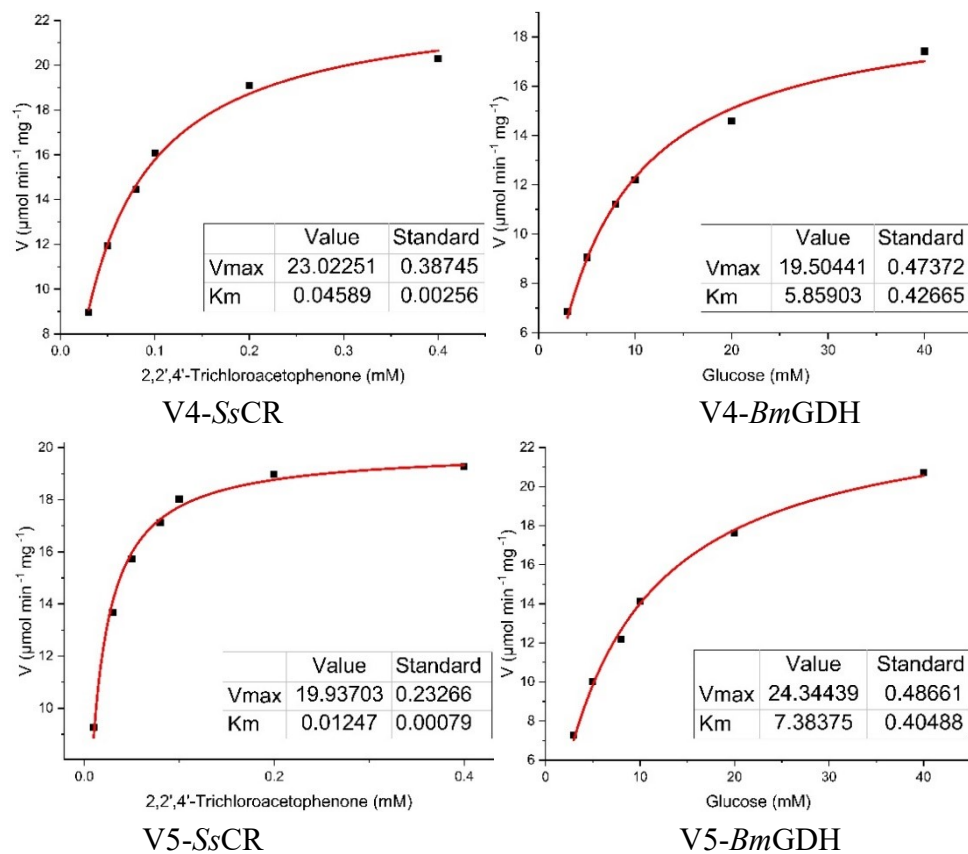


Figure S8. Michaelis-Menten kinetic assessments of *SsCR* and *BmGDH* in V0-V5.

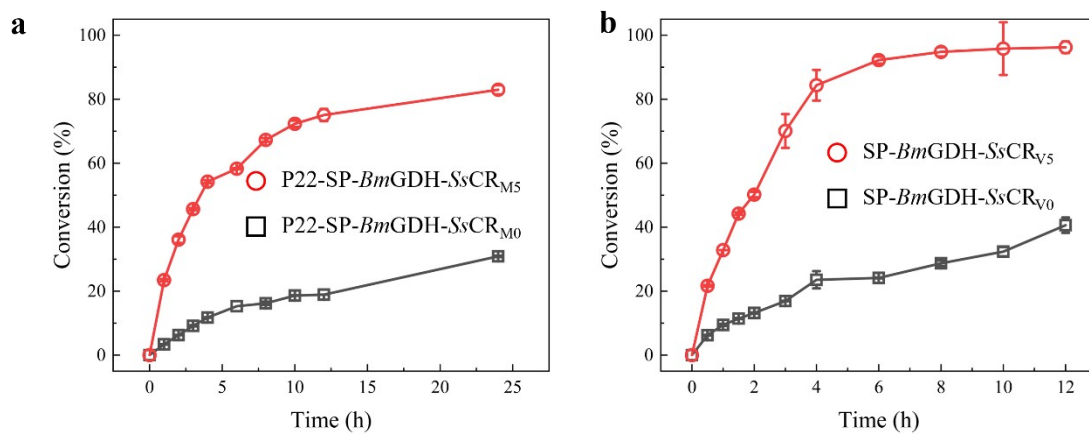


Figure S9. Conversion of **1a** by the nanoreactors P22-SP-*BmGDH-SsCR* (M0 and M5) and the fusion proteins SP-*BmGDH-SsCR* (V0 and V5). (a) The time-course conversion of 10 mM **1a** by P22-SP-*BmGDH-SsCR* M0 and M5 with 10 μ M NADPH cofactor concentration. (b) The time-course conversion of 10 mM **1a** by SP-*BmGDH-SsCR* V0 and V5.

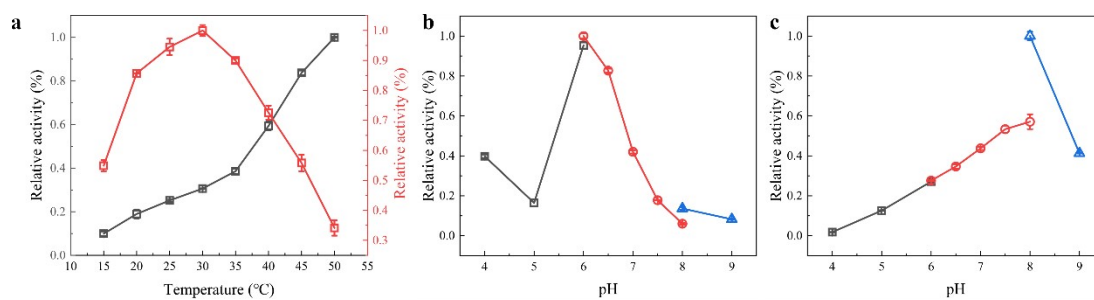


Figure S10. Characterization of P22-SP-*BmGDH-SsCR* M0. (a) Characterization of the optimal reaction temperature of *SsCR* (red square) and *BmGDH* (black square) encapsulated in M0. (b) Characterization of the optimal reaction pH of *SsCR* encapsulated in M0 (black square: sodium citrate buffer; Red circle: sodium phosphate buffer; Blue triangle: Tris – HCl buffer). (c) Characterization of the optimal reaction pH of *BmGDH* encapsulated in M0 (black square: sodium citrate buffer; Red circle: sodium phosphate buffer; Blue triangle: Tris – HCl buffer).

Table S1. Catalytic efficiency of M0 variants toward **1a** and glucose

Entry	Mutants	Mutations	$k_{\text{cat}}/K_{\text{m}}$	Fold	$k_{\text{cat}}/K_{\text{m}}$	Fold
			<i>SsCR</i> ($\text{s}^{-1} \text{mM}^{-1}$)		<i>BmGDH</i> ($\text{s}^{-1} \text{mM}^{-1}$)	
1	M0	-	375.0 ± 416.8	1.0	0.113 ± 0.007	1.0
2	M1	V356A	723.4 ± 250.5	1.9	0.197 ± 0.017	1.7
3	M1-1	T208A	477.8 ± 214.5	1.3	0.928 ± 0.019	0.82
4	M1-2	L209S	656.7 ± 358.4	1.8	0.103 ± 0.059	0.91

Table S2. Turnover frequency of SP-*Bm*GDH-*Ss*CR variants with **1a** and glucose.

Entry	Enzyme	Mutations	[1a] (mM)	Glucose (mM)	NADP ⁺ (mM)	Conv [%] ^[b]	TOF [min ⁻¹] ^[c]	Folds
1	V0	-	1	10	1	4.0	1.1×10^2	1
2	V1	V356A	1	10	1	5.1	1.5×10^2	1.3
3	V2	V356A/L211H	1	10	1	12.7	3.6×10^2	3.2
4	V3	V356A/L211H/S743G	1	10	1	12.4	3.5×10^2	3.1
5	V4	V356A/L211H/S743G/S445H	1	10	1	14.0	4.0×10^2	3.5
6	V5	V356A/L211H/S743G/S445H/V193 T	1	10	1	7.3	2.0×10^2	1.8

[a] Reaction conditions: using 0.1 mg SP-*Bm*GDH-*Ss*CR, PBS (10 mL, 100 mM, pH 6.0), 20 vol % DMSO at room temperature (30 °C). [b] GC conversion to **2a** at 1 h. [c] P22-*Bm*GDH-*Ss*CR turnover frequency (mol **1a** converted per mol SP-*Bm*GDH-*Ss*CR per min) was calculated after 60 minutes.

Table S3. Michaelis-Menten kinetic analysis of *SsCR* and *BmGDH* in M0–M5.

Entry	Mutants	Mutations	k_{cat} (s ⁻¹)	K_{m} (mM)	$k_{\text{cat}}/K_{\text{m}}$	Fold ^a	k_{cat} (s ⁻¹)	K_{m} (mM)	$k_{\text{cat}}/K_{\text{m}}$	Fold ^b
					<i>SsCR</i> (s ⁻¹ mM ⁻¹)				<i>BmGDH</i> (s ⁻¹ mM ⁻¹)	
1	M0	-	39.7 ± 26.6	0.106 ± 0.094	375.0 ± 416.8	1.0	1.001 ± 0.023	8.866 ± 0.520	0.113 ± 0.007	1.0
2	M1	V356A	13.7 ± 1.6	0.019 ± 0.006	723.4 ± 250.5	1.9	1.367 ± 0.041	6.925 ± 0.577	0.197 ± 0.017	1.7
3	M2	V356A/L211H	10.4 ± 0.3	0.075 ± 0.005	138.3 ± 9.8	0.4	1.397 ± 0.036	6.912 ± 0.503	0.202 ± 0.016	1.8
4	M3	V356A/L211H / S743G	11.3 ± 0.4	0.058 ± 0.007	195.0 ± 24.7	0.5	1.297 ± 0.024	6.409 ± 0.346	0.203 ± 0.012	1.8
5	M4	V356A/L211H /S743G/S445H	11.4 ± 0.3	0.056 ± 0.005	203.0 ± 17.3	0.5	1.510 ± 0.015	6.184 ± 0.186	0.244 ± 0.008	2.2
6	M5	V356A/L211H /S743G/S445H/V193T	8.1 ± 0.1	0.016 ± 0.001	517.3 ± 36.2	1.4	1.473 ± 0.024	4.925 ± 0.255	0.299 ± 0.016	2.6

^aFold: $k_{\text{cat}}/K_{\text{m}}$ of *SsCR* in M0–M5 compared with that of M0. ^bFold: $k_{\text{cat}}/K_{\text{m}}$ of *BmGDH* in M0–M5 compared with that of M0.

Entry	Mutants	Mutations	k_{cat} (s ⁻¹)	K_{m} (mM)	$k_{\text{cat}}/K_{\text{m}}$	Fold ^a	k_{cat} (s ⁻¹)	K_{m} (mM)	$k_{\text{cat}}/K_{\text{m}}$	Fold ^b
					<i>SsCR</i> (s ⁻¹ mM ⁻¹)				<i>BmGDH</i> (s ⁻¹ mM ⁻¹)	
1	V0	-	109.9 ± 3.6	0.011 ± 0.002	10026.8 ± 1509.8	1.0	14.5 ± 0.3	6.374 ± 0.374	2.281 ± 0.142	1.0
2	V1	V356A	138.5 ± 10.0	0.022 ± 0.004	6230.1 ± 1239.2	0.6	15.8 ± 0.3	6.543 ± 0.414	2.413 ± 0.162	1.1
3	V2	V356A/L211H	81.0 ± 0.9	0.046 ± 0.002	1773.9 ± 72.2	0.18	14.4 ± 0.4	6.870 ± 0.542	2.096 ± 0.175	0.92
4	V3	V356A/L211H /S743G	88.4 ± 1.7	0.045 ± 0.003	1952.8 ± 132.4	0.19	15.7 ± 0.2	6.428 ± 0.287	2.445 ± 0.116	1.1
5	V4	V356A/L211H /S743G/S445H	64.8 ± 1.1	0.046 ± 0.003	1412.2 ± 82.3	0.14	13.7 ± 0.3	5.859 ± 0.427	2.343 ± 0.180	1.0
6	V5	V356A/L211H /S743G/S445H/V19 3T	59.1 ± 0.7	0.012 ± 0.001	4500.3 ± 289.9	0.45	17.1 ± 0.3	7.384 ± 0.405	2.320 ± 0.135	1.0

Table S4. Michaelis-Menten kinetic analysis of SP-*BmGDH-SsCR* variants.

^aFold: k_{cat}/K_m of *SsCR* in V0–V5 compared with that of V0. ^bFold: k_{cat}/K_m of *BmGDH* variants in V0–V5 compared with that of V0.

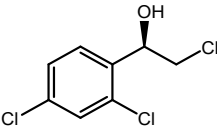
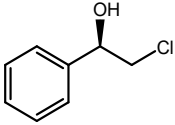
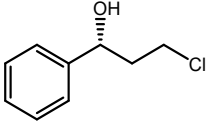
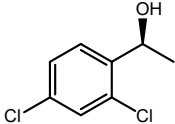
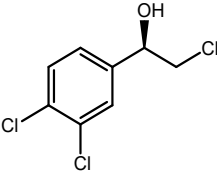
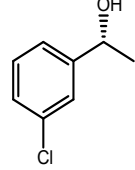
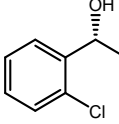
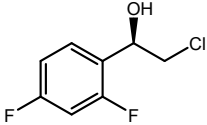
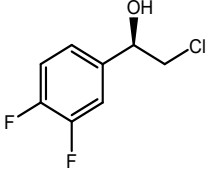
Table S5. Michaelis-Menten kinetics analysis of *BmGDH* variants.

Glucose				
Mutant	K_m (mM)	k_{cat} (s ⁻¹)	k_{cat}/K_m (s ⁻¹ mM ⁻¹)	Folds
WT	7.717 ± 0.572	32.89 ± 0.90	4.262 ± 0.337	1.0
V11A (V356A)	10.948 ± 0.982	44.65 ± 1.68	4.078 ± 0.397	0.95
V11A (V356A)/S100H (S445H)	6.252 ± 0.294	35.04 ± 0.56	5.605 ± 0.279	1.3

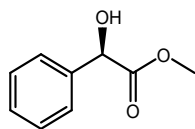
Table S6. Michaelis-Menten kinetics analysis of *SsCR* variants.

2,2,4'-trichloroacetophenone				
Mutant	K_m (mM)	k_{cat} (s ⁻¹)	k_{cat}/K_m (s ⁻¹ mM ⁻¹)	Folds
WT	0.015 ± 0.002	103.8 ± 4.8	6808.1 ± 1057.1	1.0
L211H	0.053 ± 0.003	57.4 ± 0.9	1090.5 ± 58.9	0.16
V193T/L211H	0.021 ± 0.001	45.2 ± 0.7	2145.9 ± 154.5	0.32

Table S7. GC conditions used to determine the enantioselectivity of products.

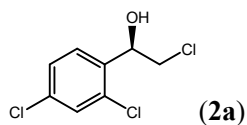
Entry	Product	Enantioselectivity determination
2a		GC column temperature: 150°C hold for 6 min, 20°C/min to 180 °C
2b		GC column temperature: 120°C, 2°C/min to 128°C 13 min, 20°C/min to 180°C 3 min
2c		GC column temperature: 100°C hold for 4 min, 5°C/min to 150 °C, 150°C hold for 10 min
2d		GC column temperature: 150°C hold for 6 min, 20°C/min to 180 °C, 180°C hold for 10 min
2e		GC column temperature: 2°C/min from 160°C to 170°C, 170°C hold for 2 min, 1°C/min from 170°C to 180°C, 180°C hold for 15 min
2f		GC column temperature: 140°C hold for 25 min
2g		GC column temperature: 140°C hold for 25 min
2h		GC column temperature: 150°C hold for 6 min, 20°C/min to 180 °C
2i		GC column temperature: 150°C hold for 6 min, 20°C/min to 180 °C

2j

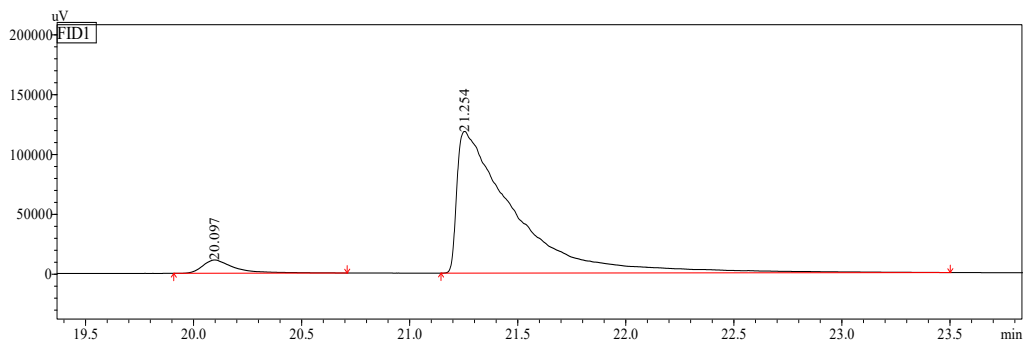


GC column temperature: 140°C hold for
25 min

2. GC spectra

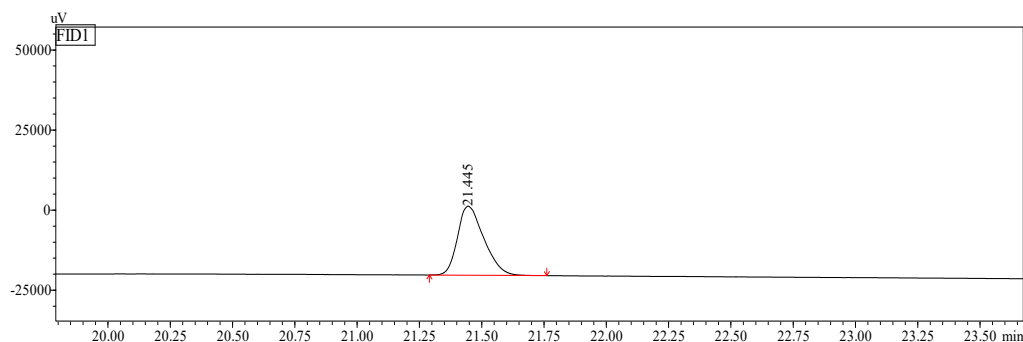


Racemic mixture of 2a



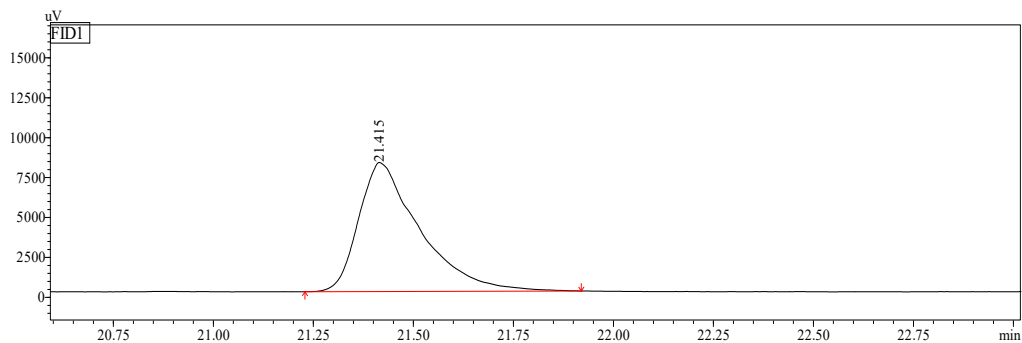
Peak#	Ret. Time(min)	Height(uV)	Area(uV*s)	Area%
1	20.097	11112	113966	8.6
2	21.254	118306	2182124	91.4

Reduction with M5

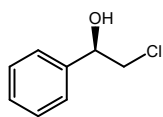


Peak#	Ret. Time(min)	Height(uV)	Area(uV*s)	Area%
1	21.445	21542	158370	100

Reduction with M0

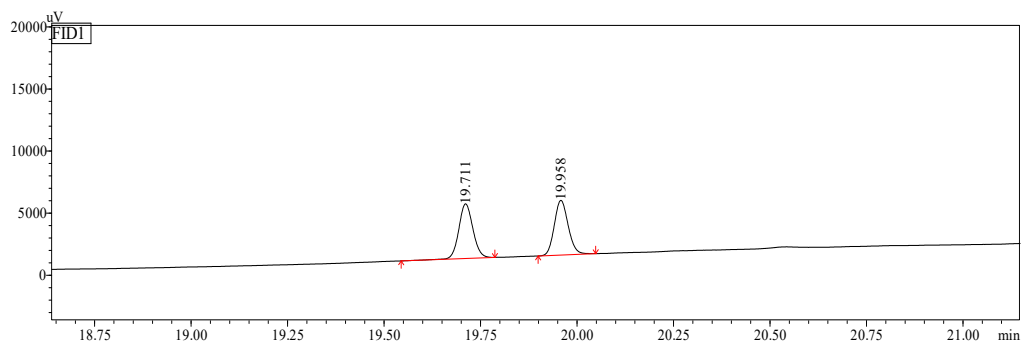


Peak#	Ret. Time(min)	Height(uV)	Area(uV*s)	Area%
1	21.415	8070	85657	100



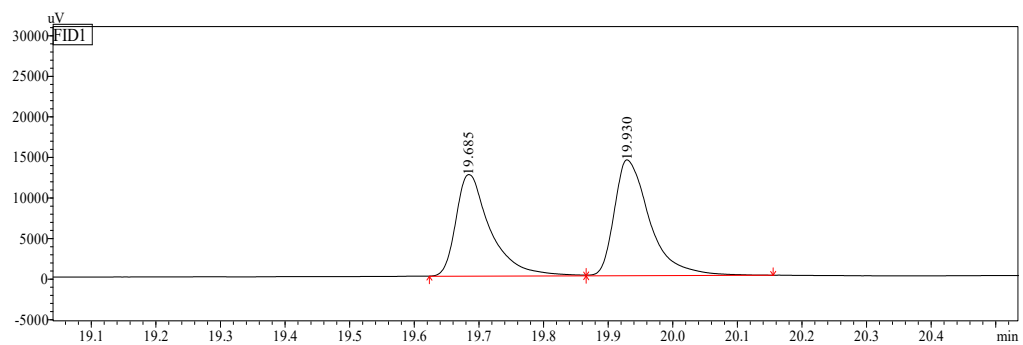
(2b)

Racemic mixture of **2b**



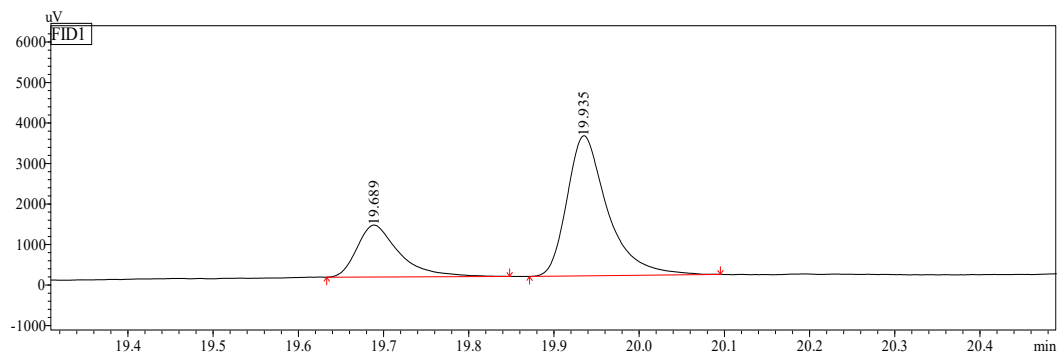
Peak#	Ret. Time(min)	Height(uV)	Area(uV*s)	Area%
1	19.711	4380	11187	50.4
2	19.958	4387	11002	49.6

Reduction with M5

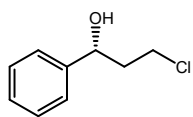


Peak#	Ret. Time(min)	Height(uV)	Area(uV*s)	Area%
1	19.685	12456	46543	46.2
2	19.930	14252	54229	53.8

Reduction with M0

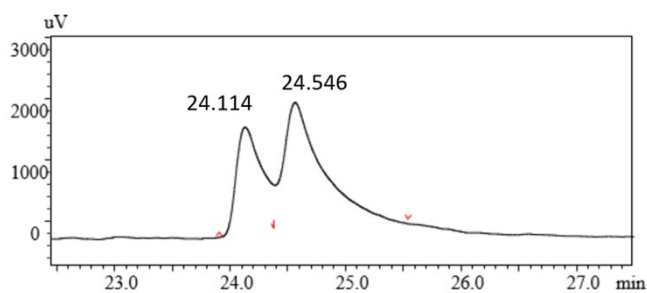


Peak#	Ret. Time(min)	Height(uV)	Area(uV*s)	Area%
1	19.689	1274	4403	27.8
2	19.935	3448	11430	72.2



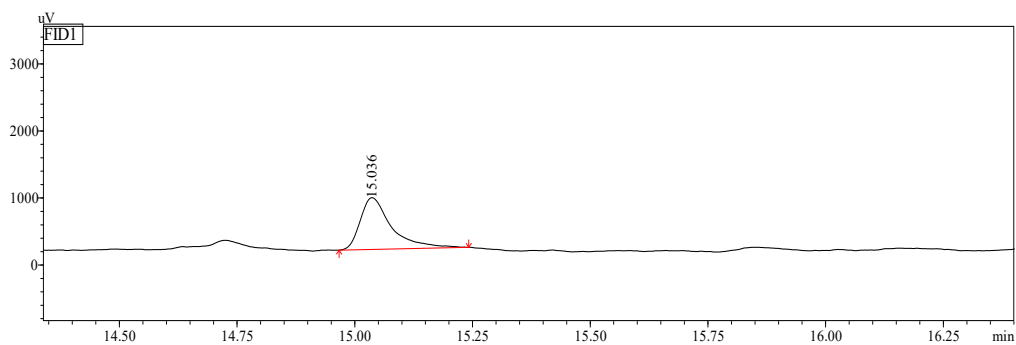
(2c)

Racemic mixture of 2c



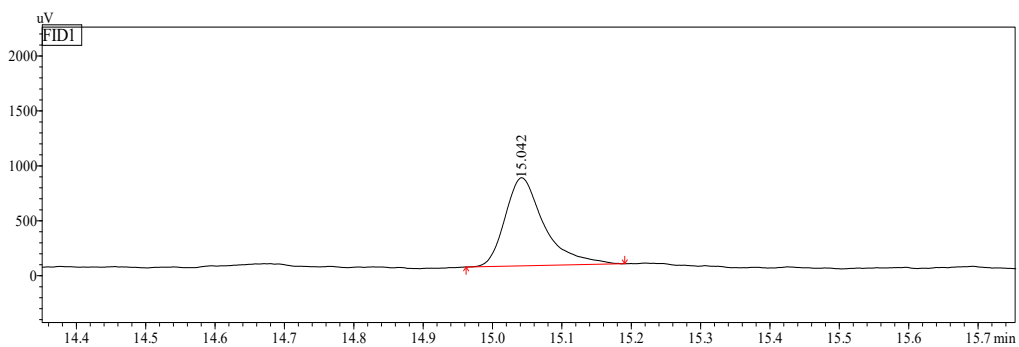
Peak#	Ret. Time(min)	Height(uV)	Area(uV*s)	Area%
1	24.114	1763	28246	35.2
2	24.546	2114	52030	64.8

Reduction with M5

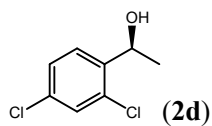


Peak#	Ret. Time(min)	Height(uV)	Area(uV*s)	Area%
1	15.036	769	3558	100

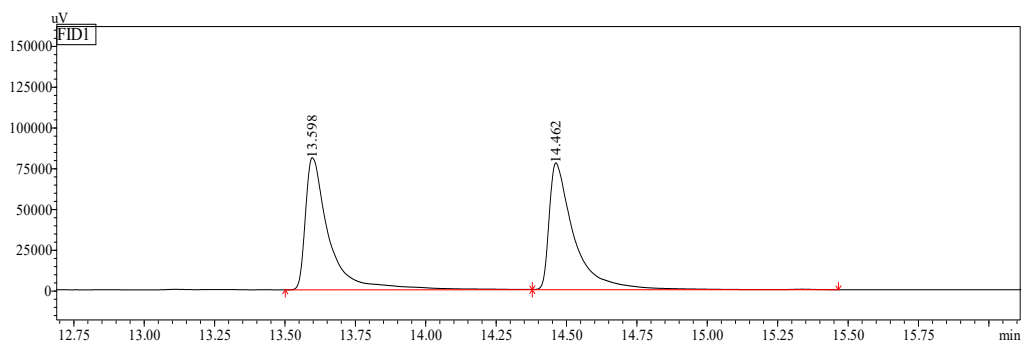
Reduction with M0



Peak#	Ret. Time(min)	Height(uV)	Area(uV*s)	Area%
1	15.042	798	3139	100

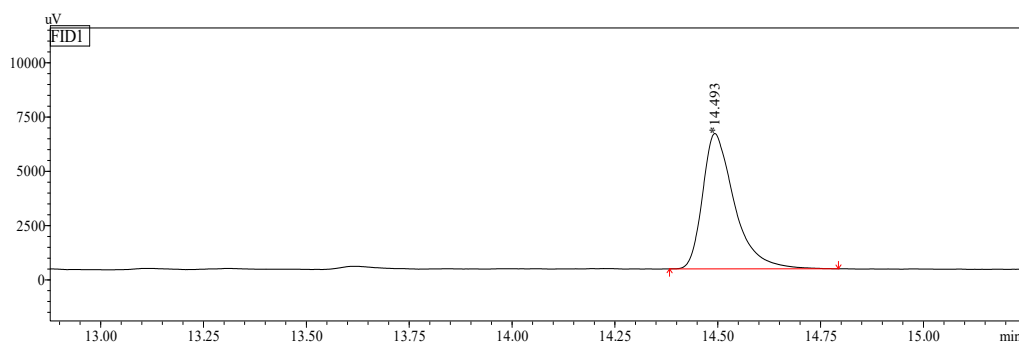


Racemic mixture of **2d**



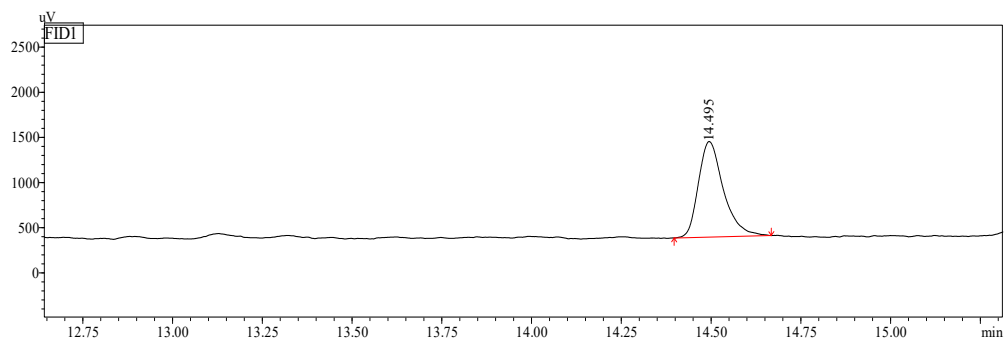
Peak#	Ret. Time(min)	Height(uV)	Area(uV*s)	Area%
1	13.598	80963	476459	49.9
2	14.462	77522	479036	50.1

Reduction with M5

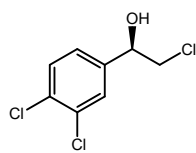


Peak#	Ret. Time(min)	Height(uV)	Area(uV*s)	Area%
1	14.493	6228	33501	100

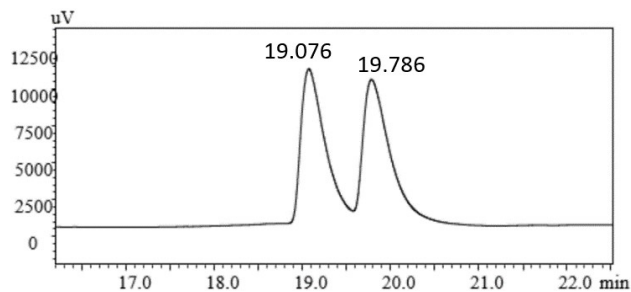
Reduction with M0



Peak#	Ret. Time(min)	Height(uV)	Area(uV*s)	Area%
1	14.495	1056	5136	100

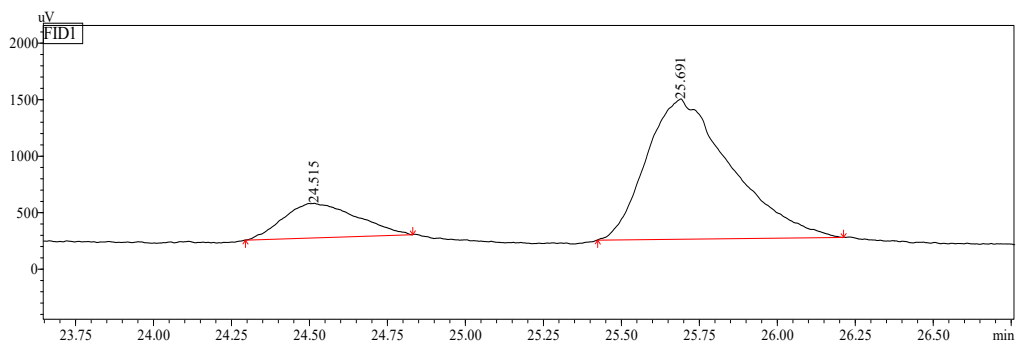


Racemic mixture of **2e**



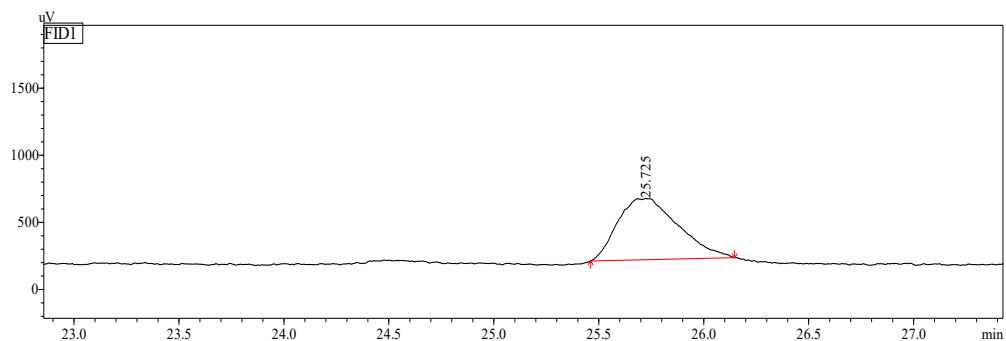
Peak#	Ret. Time(min)	Height(uV)	Area(uV*s)	Area%
1	19.076	10469	202986	48.5
2	19.786	9785	214919	51.5

Reduction with M5

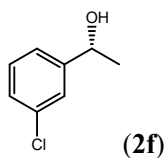


Peak#	Ret. Time(min)	Height(uV)	Area(uV*s)	Area%
1	24.515	305	5015	17.6
2	25.691	1239	23434	82.4

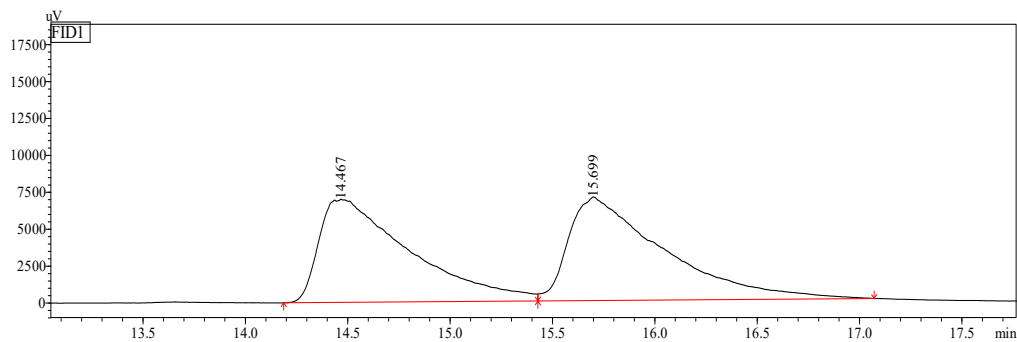
Reduction with M0



Peak#	Ret. Time(min)	Height(uV)	Area(uV*s)	Area%
1	25.725	456	9165	100

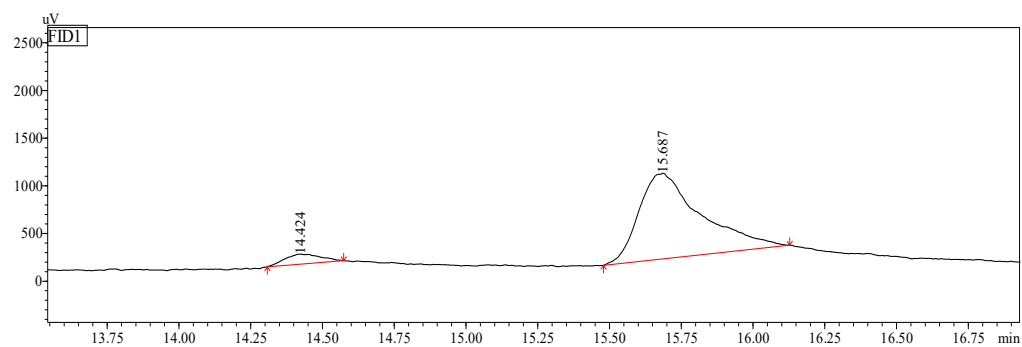


Racemic mixture of **2f**



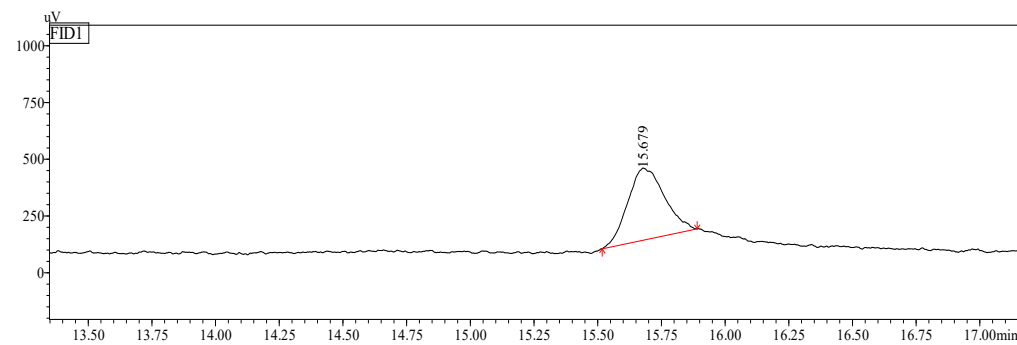
Peak#	Ret. Time(min)	Height(uV)	Area(uV*s)	Area%
1	14.467	6976	215158	48.7
2	15.699	7009	226422	51.3

Reduction with M5

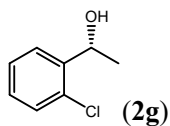


Peak#	Ret. Time(min)	Height(uV)	Area(uV*s)	Area%
1	14.424	104	900	6.2
2	15.687	898	13542	93.8

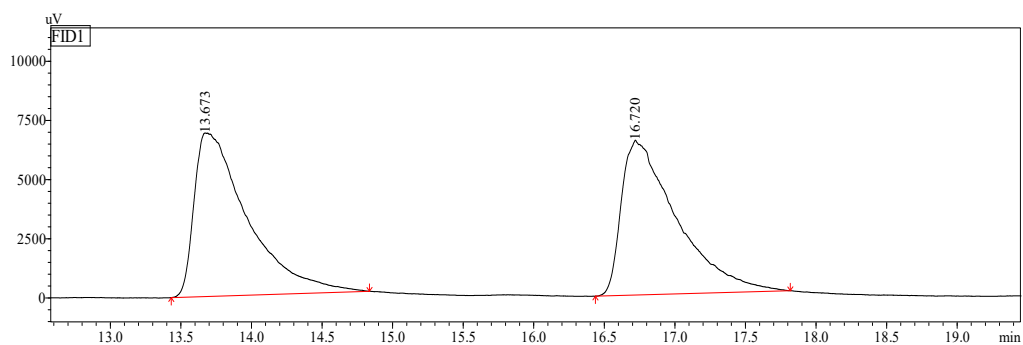
Reduction with M0



Peak#	Ret. Time(min)	Height(uV)	Area(uV*s)	Area%
1	15.679	317	3174	100

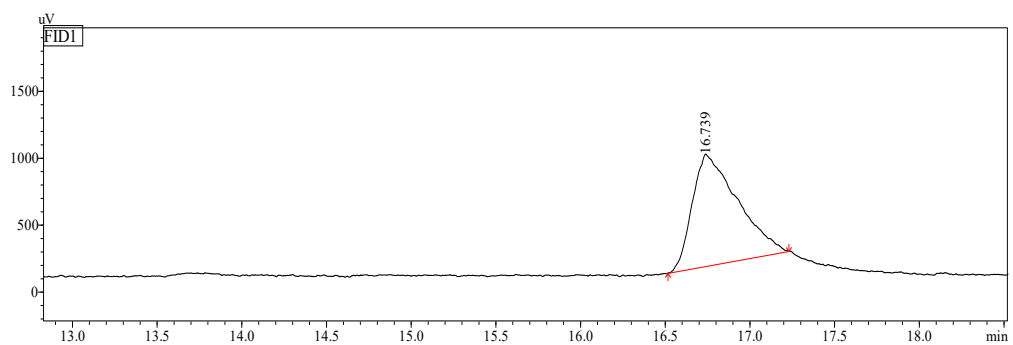


Racemic mixture of 2g



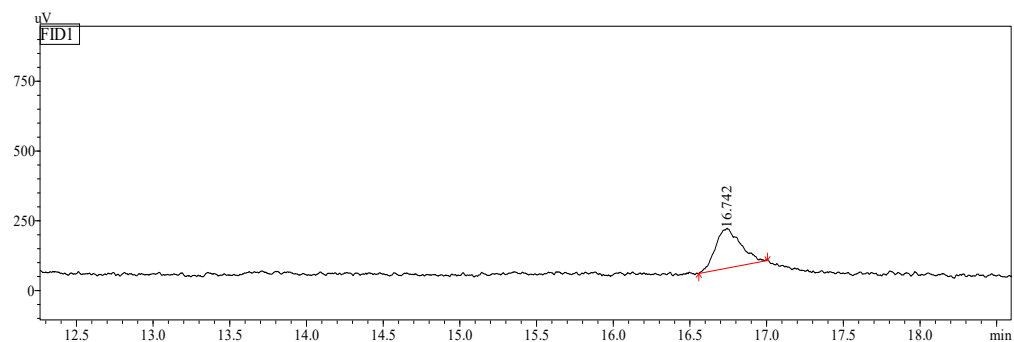
Peak#	Ret. Time(min)	Height(uV)	Area(uV*s)	Area%
1	13.673	6907	181142	50.5
2	16.720	6541	177697	49.5

Reduction with M5

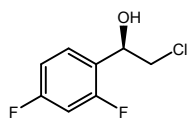


Peak#	Ret. Time(min)	Height(uV)	Area(uV*s)	Area%
1	16.739	839	15502	100

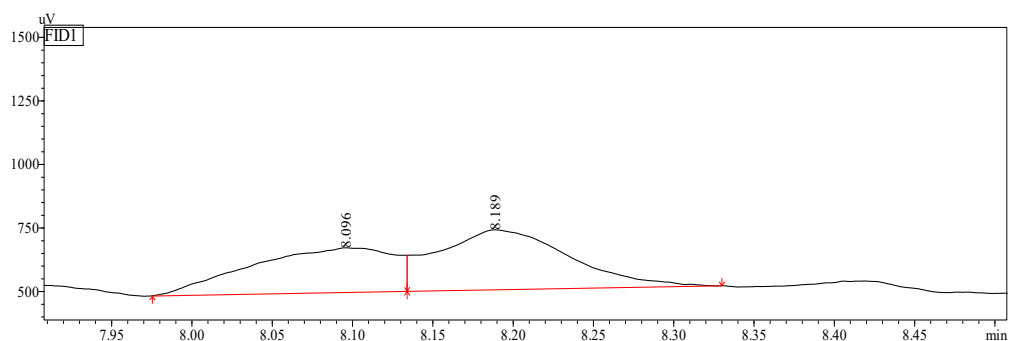
Reduction with M0



Peak#	Ret. Time(min)	Height(uV)	Area(uV*s)	Area%
1	16.742	143	1640	100

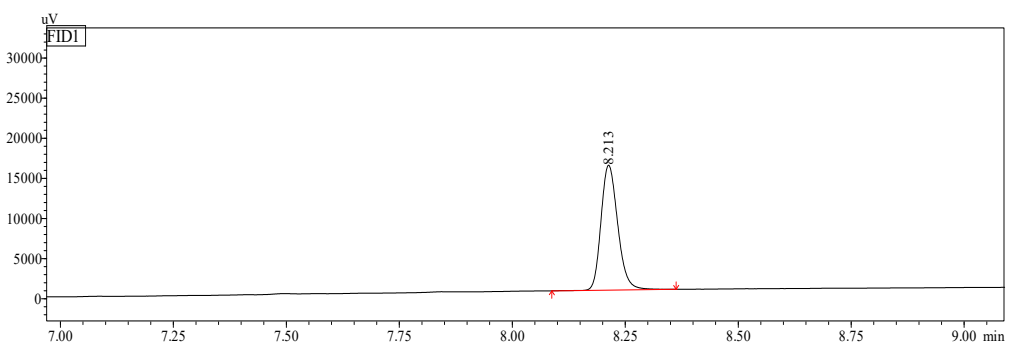


Racemic mixture of 2h



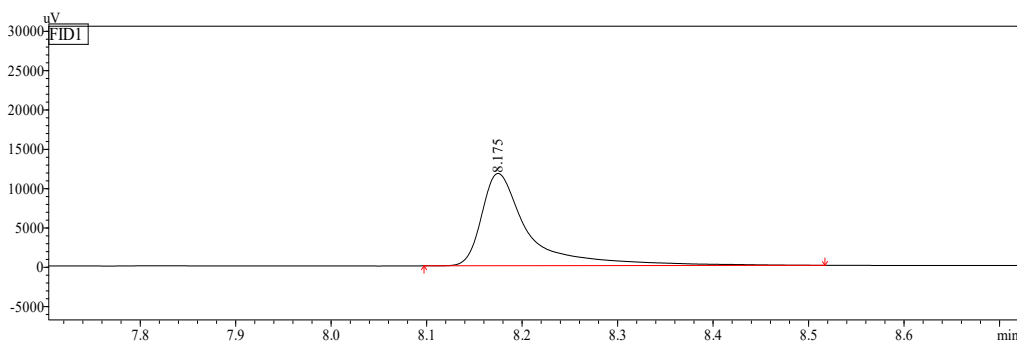
Peak#	Ret. Time(min)	Height(uV)	Area(uV*s)	Area%
1	8.096	176	1099	45.0
2	8.189	236	1348	55.0

Reduction with M5

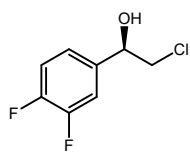


Peak#	Ret. Time(min)	Height(uV)	Area(uV*s)	Area%
1	8.213	15445	40203	100

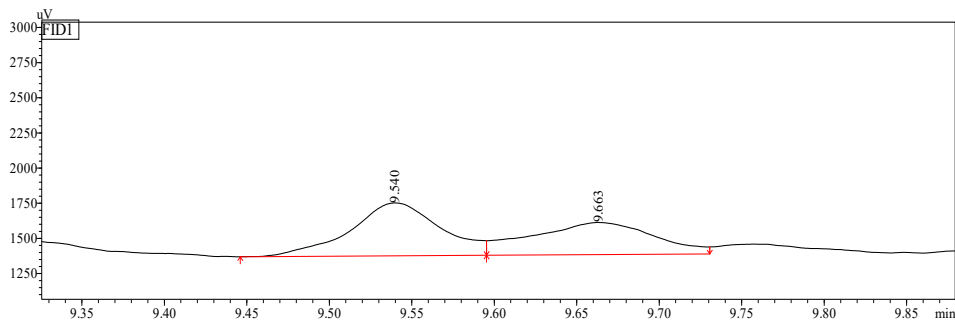
Reduction with M0



Peak#	Ret. Time(min)	Height(uV)	Area(uV*s)	Area%
1	8.175	11696	40136	100

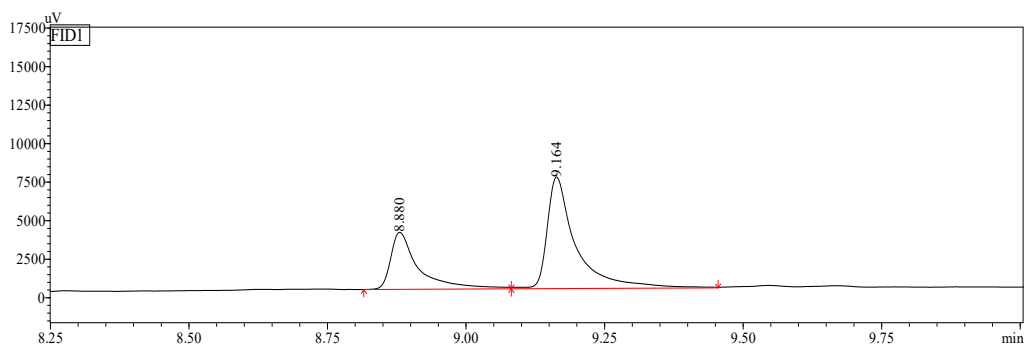


Racemic mixture of 2i



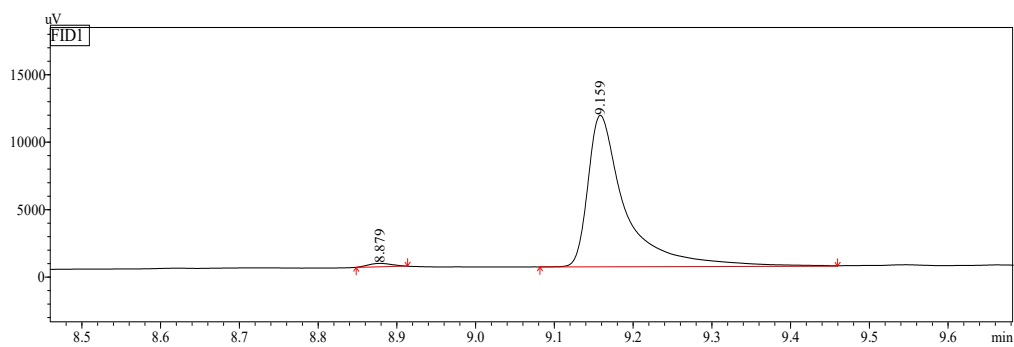
Peak#	Ret. Time(min)	Height(uV)	Area(uV*s)	Area%
1	9.540	374	1431	54.8
2	9.663	228	1182	45.2

Reduction with M5

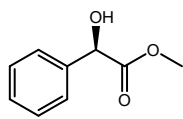


Peak#	Ret. Time(min)	Height(uV)	Area(uV*s)	Area%
1	8.880	3677	13027	33.1
2	9.164	7221	26293	66.9

Reduction with M0

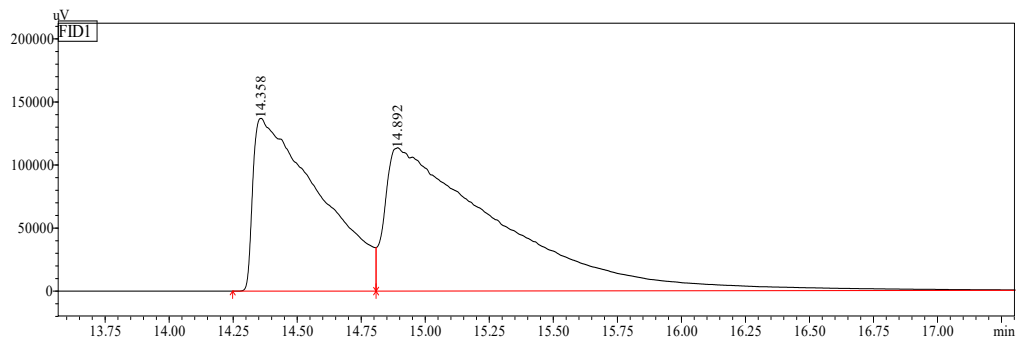


Peak#	Ret. Time(min)	Height(uV)	Area(uV*s)	Area%
1	8.879	252	532	1.4
2	9.159	11185	37528	98.6



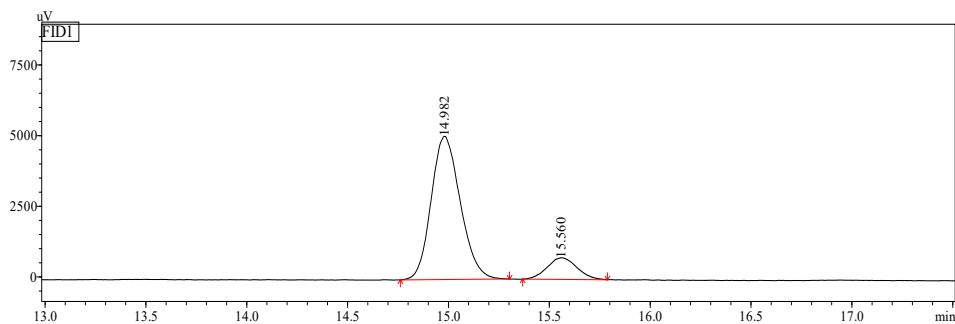
(2j)

Racemic mixture of 2j



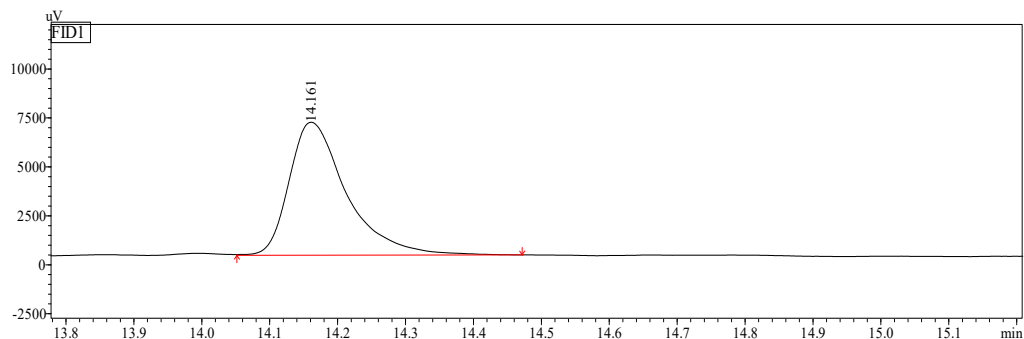
Peak#	Ret. Time(min)	Height(uV)	Area(uV*s)	Area%
1	14.358	136945	2477258	41.0
2	14.892	113459	3562963	59.0

Reduction with M5



Peak#	Ret. Time(min)	Height(uV)	Area(uV*s)	Area%
1	14.982	5064	50961	86.6
2	15.560	765	7874	13.4

Reduction with M0



Peak#	Ret. Time(min)	Height(uV)	Area(uV*s)	Area%
1	14.161	6788	39848	100